

Merging time-scales of stellar subclumps in young star-forming regions

M. Fellhauer,^{1,2*} M. I. Wilkinson³ and P. Kroupa⁴

¹*Institute of Astronomy, University of Cambridge, Madingley Road, Cambridge CB3 0HA*

²*Departamento de Astronomia, Universidad de Concepcion, Casila 160-C, Concepcion, Chile*

³*Department of Physics and Astronomy, University of Leicester, University Road, Leicester LE1 7RH*

⁴*Argelander-Institut für Astronomie, Universität Bonn, Auf dem Hügel 71, 53121 Bonn, Germany*

Accepted 2009 May 1. Received 2009 April 20; in original form 2009 February 18

ABSTRACT

Recent observations and hydrodynamical simulations of star formation inside a giant molecular cloud have revealed that, within a star-forming region, stars do not form evenly distributed throughout this region, but rather in small subclumps. It is generally believed that these subclumps merge and form a young star cluster. The time-scale of this merging process is crucial for the evolution and the possible survival of the final star cluster. The key issue is whether this merging process happens faster than the time needed to remove the residual gas of the cloud. A merging time-scale shorter than the gas-removal time would enhance the survival chances of the resulting star cluster. In this paper, we show by means of numerical simulations that the time-scale of the merging is indeed very fast. Depending on the details of the initial subclump distribution, the merging may occur before the gas is expelled from the newly formed cluster via either supernovae or the winds from massive stars. Our simulations further show that the resulting merger objects have a higher effective star formation efficiency than the overall star-forming region and confirm the results that mass-segregated subclumps form mass-segregated merger objects.

Key words: methods: *N*-body simulations – stars: formation – galaxies: star clusters.

1 INTRODUCTION

The formation and survival of young, embedded star clusters is an important issue not only for the star cluster community but also has implications for our understanding of the formation and evolution of galaxies as a whole. Stars are now believed to form mostly in star clusters, which later dissolve and distribute their stars to their host galaxy.

In recent years, considerable progress in our understanding of the star formation process has been made and a general picture is emerging. Star clusters form out of collapsing cloud clumps in molecular clouds (Tilley & Pudritz 2004). These collapses are triggered by turbulent fragmentation of clouds and their clumps (MacLow & Klessen 2004). The clumps are observed to be aligned in filamentary structures that can be reproduced by supersonic turbulent simulations and they contain many cores (Burkert & Bodenheimer 2000; Klessen & Burkert 2001). Each core forms a single star or a binary. The mass function found for these cores is essentially the same as the initial mass function of the stars (Johnstone et al. 2000; Goodwin et al. 2008). The cores are themselves clumped in small subclumps containing a few to a few tens of stars (Bonnell, Bate & Vine 2003). While the star formation efficiency [SFE; i.e.

the fraction of gas which ends up in the star(s)] in these cores is high, the overall SFE measured over the whole molecular cloud is very low, of the order of a few per cent (Clark & Bonnell 2004) and ≤ 40 per cent in cluster-forming clumps (i.e. embedded star clusters; Lada & Lada 2003).

The remaining gas does not stay in the newborn star cluster but is driven outwards by stellar feedback. In embedded clusters containing more than a few hundred stars, the feedback consists of photoionizing radiation, the winds of high-mass stars and finally the onset of the first supernova explosions (Goodwin 1997). For such clusters, the feedback energy can easily be sufficient to unbind the gas leading to a gas expulsion phase which is rather short, comparable to the crossing time of the star cluster (Kroupa 2005). Pictures of young massive star clusters, for example in the central region of the Antennae (NGC 4038/4039; Whitmore et al. 1999), reveal that they are already surrounded by H α bubbles stemming from the gas which was blown out of the star cluster. It has been shown that these star clusters can be as young as 5–6 Myr. The outflow velocities of the gas have been measured to be 25–30 km s^{−1} (Whitmore et al. 1999), which corresponds to gas-evacuation times of 0.2 Myr for cluster radii of 4 pc. This is comparable to the crossing time of a $10^5 M_{\odot}$ cluster. As a result of this strong and rapid mass loss, the star cluster is left out of virial equilibrium. The velocities of the stars are too high for the reduced mass of the star cluster. Hence, even more mass is lost when stars escape from the star cluster. This

*E-mail: mfellhauer@astro-udec.cl

may finally lead to the complete dissolution of the cluster (also called ‘infant mortality’; e.g. de Grijs & Goodwin 2008; Gieles & Bastian 2008). But if the SFE is as high as 33 per cent or above, a small bound core remains (Goodwin 1997; Adams 2000; Boily & Kroupa 2003a,b) which may account for the survival of low-mass, Pleiades-type clusters (Kroupa, Aarseth & Hurley 2001). Geyer & Burkert (2001) argue that the SFE has to be larger than 50 per cent to get a bound core but if the stars have almost no initial velocity dispersion then a SFE of 10 per cent could suffice. This means that the measurement of the initial velocity distribution in newborn embedded star clusters will be crucial to find out whether, and how, star clusters survive.

All these authors imply that a spherical embedded cluster has already formed before the remaining gas is blown out of the star-forming region. In this paper, we want to investigate if this assumption is valid. We start at the stage when the subclumps have formed (at the endpoint of hydrodynamical smoothed particle hydrodynamics simulations), but the stars are still in their formation process and therefore have not started to blow away the remaining gas. Once the stars start to shine, their stellar winds blow away the residual gas. This gas removal happens on very short time-scales, but is longer for more massive gas cores at a given SFE (Parmentier et al. 2008). For clusters with masses of less than $10^5 M_\odot$, this gas-removal time is shorter than the crossing time of the embedded star cluster (Baumgardt, Kroupa & Parmentier 2008). For massive star clusters, the explosion of the first supernova will remove the residual gas. This is in principle a different ansatz than most of the numerical studies so far (e.g. Goodwin 1998; Scally & Clarke 2002; Goodwin & Whitworth 2004; McMillan, Vesperini & Portegies Zwart 2007), which start with a (mostly cold) clumpy structure without the gaseous background.

In this paper, we try to answer the following, related, questions: is there sufficient time before the gas is driven out for the subclumps to merge and form a spherical, embedded cluster? If so, what is the effective SFE of these embedded clusters? By means of numerical simulations, we investigate the time-scale of this merging process.

2 SETUP

The setup of our simulations is based on a typical outcome of hydrodynamical simulations of a star-forming region inside a giant molecular cloud (Bonnell et al. 2003). We model the star-forming region as a Plummer sphere with a mass of $M_{sc} = M = 1000 M_\odot$ and a Plummer radius $R_{pl}^{sc} = 0.2$ pc. We assume that in this cloud stars have formed in small subclumps with an overall SFE $\epsilon = 0.32$. This gives us $320 M_\odot$ in stars, which we divide into $N_0 = 16$ subclumps of $M_{cl} = 20 M_\odot$. Each of these subclumps is modelled as a small Plummer sphere with a Plummer radius of $R_{pl} = 0.01$ pc and a cut-off radius of $R_{cut} = 0.05$ pc. These clumps are distributed themselves according to the Plummer distribution function of the whole gas cloud taking a cut-off radius of 1 pc. Because we do not consider the hydrodynamics of the gas, the remaining mass in gas is modelled as a time-varying analytical background Plummer potential. The potential is kept constant except when stated otherwise.

To put the results of this model (our standard model) into context, we also perform a parameter study, in which we vary R_{pl}^{sc} , N_0 and ϵ . For clarity, we give the parameters of our standard model as well as for the comparison runs in Table 1.

The study of the merging behaviour of these subclumps suffers heavily from the low-number statistics ($N_0 = 16$). For each set of parameters, we therefore run up to five simulations starting from different random realizations and calculate the average of the results.

Table 1. Table of the initial parameters of our simulations.

α	ϵ	N_0	R_{pl}^{sc} (pc)	R_{cut}^{sc} (pc)	M_{pl}^{sc} (M_\odot)	T_{cr}^{sc} (kyr)	σ_{3D}^{sc} (km s^{-1})	M_{star} (M_\odot)	M_{gas} (M_\odot)	R_{pl} (pc)	R_{cut} (pc)	M_{pl} (M_\odot)	T_{cr} (kyr)	σ_{3D} (km s^{-1})
0.05	0.32	16	0.20	1.00	1000	260	2.5	320	680	0.01	0.05	20.0	20	1.6
0.01	0.32	16	1.00	5.00	1000	2950	1.1	320	680	0.01	0.05	20.0	20	1.6
0.02	0.32	16	0.50	2.50	1000	1043	1.6	320	680	0.01	0.05	20.0	20	1.6
0.10	0.32	16	0.10	0.50	1000	93	3.6	320	680	0.01	0.05	20.0	20	1.6
0.20	0.32	16	0.05	0.25	1000	33	5.0	320	680	0.01	0.05	20.0	20	1.6
0.50	0.32	16	0.02	0.10	1000	8	8.0	320	680	0.01	0.05	20.0	20	1.6
0.05	0.32	4	0.20	1.00	1000	260	2.5	320	680	0.01	0.05	80.0	10	3.2
0.05	0.32	8	0.20	1.00	1000	260	2.5	320	680	0.01	0.05	40.0	15	2.3
0.05	0.32	32	0.20	1.00	1000	260	2.5	320	680	0.01	0.05	10.0	29	1.1
0.05	0.10	16	0.20	1.00	1000	260	2.5	100	900	0.01	0.05	6.3	37	0.9
0.05	0.20	16	0.20	1.00	1000	260	2.5	200	800	0.01	0.05	12.5	26	1.3
0.05	0.25	16	0.20	1.00	1000	260	2.5	250	750	0.01	0.05	15.6	24	1.4
0.05	0.50	16	0.20	1.00	1000	260	2.5	500	500	0.01	0.05	31.3	17	2.0
0.05	0.60	16	0.20	1.00	1000	260	2.5	600	400	0.01	0.05	37.5	15	2.2
0.05	0.70	16	0.20	1.00	1000	260	2.5	700	300	0.01	0.05	43.8	14	2.4
0.05	1.00	16	0.20	1.00	1000	260	2.5	1000	0	0.01	0.05	62.5	12	2.8
0.10	0.10	16	0.10	0.50	1000	93	3.6	100	900	0.01	0.05	6.3	37	0.9
0.10	0.20	16	0.10	0.50	1000	93	3.6	200	800	0.01	0.05	12.5	26	1.3
0.10	0.25	16	0.10	0.50	1000	93	3.6	250	750	0.01	0.05	15.6	24	1.4
0.10	0.50	16	0.10	0.50	1000	93	3.6	500	500	0.01	0.05	31.3	17	2.0
0.10	0.70	16	0.10	0.50	1000	93	3.6	700	300	0.01	0.05	43.8	14	2.4
0.10	1.00	16	0.10	0.50	1000	93	3.6	1000	0	0.01	0.05	62.5	12	2.8

Note. The first line shows the parameters of our standard model. The columns give the filling factor α , the SFE ϵ and the number of subclumps N_0 , followed by the Plummer radius, the cut-off radius, the total mass, the crossing time and the velocity dispersion of the star-forming region. The next two columns denote the mass in stars and the mass in gas (modelled as analytical background). Finally, we show the Plummer radius, the cut-off radius, the mass, the crossing time and the velocity dispersion of each single clump.

We use the particle-mesh code *SUPERBOX* (Fellhauer et al. 2000) to perform the simulations. This code has the advantage that we can use an arbitrarily high particle number to model each subclump, because the particles in a collision-less code like *SUPERBOX* represent phase-space elements rather than single stars. We therefore model each clump with 100 000 particles. Furthermore, *SUPERBOX* offers two levels of high-resolution subgrids which stay focused on each object (i.e. subclump) and give us the resolution needed to follow the merging process in detail and to access the time-scales.

As with all particle-mesh codes, developed to simulate galaxies, the effects of two-body relaxation in our code are almost completely suppressed. However, we note that the internal relaxation times of our subclumps are rather low and of the order of a few kyr (7300 yr in the standard model). Although this implies that the life-times of those subclumps are very short, they will still be larger than the time needed to have a first passage through the centre of our star-forming region, i.e. the time needed to have interactions with other clumps and the central merger object. These interactions are a very violent process which will either destroy the clumps and distribute their stars in the central region or reset their internal clocks. Since internal relaxation will tend to speed up the dissolution of a star cluster, by neglecting internal processes we are therefore prolonging the merging process rather than shortening it.

A study by Sensui, Funato & Makino (2000) showed that the internal structure of galaxies does not play a role in the merging time-scales (inside a galaxy cluster) – only the distribution of galaxies inside the cluster matters. This argument should also hold for star clusters in a star cluster complex and we believe we can also apply it to the problem of this paper. The key quantities are the distribution of the relative velocities of the subclumps within the star-forming region and how much energy they can absorb with each interaction. These quantities depend only on the total masses and effective radii of the subclumps, and hence are reasonably modelled in our simulations.

Dissolving subclumps (due to the fast two-body relaxation) will distribute their stars preferentially in the centre, i.e. in and around the merger object. This process would also tend to reduce the time-scale for star cluster formation rather than prolonging it. As before, our simulations are therefore conservative as they provide an upper limit to the total amount of time required to form the merger object.

We are aware that there are also a lot of stars which are ejected from the clumps with high velocities due to close encounters within the subclumps and are subsequently lost to the forming star cluster. However, these stars only constitute a small fraction of the total stellar content of the subclumps.

We are therefore confident that the conclusions from our simplified approach to this problem will also hold for more sophisticated models, including two-body relaxation, which we plan to carry out in the future.

To make the comparison with previous work (Fellhauer et al. 2002) easier, we try to adopt the same notation of dimensionless parameters and define as a measure of the concentration of the subclumps in the gas cloud (filling factor)

$$\alpha = \frac{R_{\text{pl}}^{\text{clump}}}{R_{\text{pl}}^{\text{sc}}}. \quad (1)$$

We omit the index^{clump} in the following text. We furthermore define a dimensionless time as

$$\tau = \frac{t}{T_{\text{cr}}^{\text{sc}}}, \quad (2)$$

where $T_{\text{cr}}^{\text{sc}}$ is the crossing time of the star-forming cloud.

3 THEORETICAL BACKGROUND

A theory of merging star clusters was developed by Fellhauer et al. (2002). They investigated the merging time-scales and efficiencies of young massive star clusters forming in confined areas which they called star cluster complexes. In their case, the star clusters were merging in their own potential and not in a background potential of the residual gas. Here, we want to investigate if this theory also applies in the case of stellar subclumps forming in the potential of the residual gas inside a giant molecular cloud.

In this section, we recapitulate their theory and adapt it to our problem. Fellhauer et al. (2002) established first a velocity criterion for merging based on the work of Gerhard & Fall (1983) which reads as

$$\frac{1}{2} v_{\text{typ}}^2 \leq \frac{GM_{\text{pl}}}{R_{\text{pl}}}. \quad (3)$$

The right-hand side is a value of the order of the internal velocity dispersion of our subclumps, while the left-hand side is of the order of the clump-velocity dispersion in the star-forming region. Only if this formula is satisfied should merging between objects be possible. If we insert now $v_{\text{typ}} \approx \sqrt{2}\sigma_{\text{pl}}$ and the definitions for α and ϵ , we derive

$$\frac{N_0 \alpha}{\epsilon} \leq \frac{32}{3\pi}. \quad (4)$$

However, Fellhauer et al. (2002) noted that in simulations with large values of α the right-hand side of equation (3) has to be replaced by the unknown values of the merger object. Thus, equation (3) gives us a threshold for low-mass and low- α simulations, while in cases with a high filling factor this criterion fails.

Fellhauer et al. (2002) identified two regimes of the merging process. As long as the mean projected distance between two clusters in the centre of the cluster is smaller than the merger radius (i.e. high filling factors), the merging process is very fast, because the clusters in the centre form a central merging object almost immediately and the subsequent merging happens preferably with this object which covers a fraction η of the surface area of the star-forming region. Therefore, the subclumps merge following a ‘fast’ exponential decrease in their numbers:

$$\begin{aligned} \frac{dN}{d\tau} &= -N\eta \implies \\ N(\tau) &= N_0 \exp(-\eta\tau), \end{aligned} \quad (5)$$

where η is the fraction of the surface of the star-forming region, which is covered by the merger object and leads to a merging of the passing subclump. If time is measured in crossing times, i.e. the time the subclumps need to travel once through the star-forming region, the merger rate can be derived by simple geometrical arguments. We note that η replaces the ϵ from Fellhauer et al. (2002), which we now reserve for the SFE. Fellhauer et al. (2002) find that $\eta_F = 0.2$ in their models. This value was found to be independent of the choice of α for a wide range of values.

If the concentration of subclumps sinks below a threshold, i.e. when the mean projected distance between two clusters in the centre is larger than the merger radius, the ‘slow’ regime takes over. The subclumps still merge fast but rather with each other and build up the final merger object at later stages. Then, the merging follows

$$\begin{aligned} \frac{dN}{d\tau} &= -N \frac{(N-1)\pi r_{\text{merger}}^2}{A_{\text{sc}}} \approx \delta(\alpha) N^2 \implies \\ N(\tau) &= N_0 \frac{1}{1 + \delta(\alpha) N_0 \tau}, \end{aligned} \quad (6)$$

Table 2. Values for $\delta(\alpha)N_0$ for the different choices of the parameters used in this study.

α	ϵ	N_0	$\delta(\alpha)N_0$	$(\delta N_0)_{\text{fit}}$	η_{fit}	$t_{1/2}$ (kyr)
0.05	0.32	16	0.094	0.104 ± 0.010	0.076 ± 0.003	2500
0.01	0.32	16	0.036	0.067 ± 0.008	0.053 ± 0.004	44 000
0.02	0.32	16	0.054	0.047 ± 0.004	0.041 ± 0.002	22 000
0.10	0.32	16	0.149	0.141 ± 0.011	0.094 ± 0.004	620
0.20	0.32	16	0.241	0.380 ± 0.015	0.167 ± 0.009	87
0.50	0.32	16	0.476	2.17 ± 0.92	1.38 ± 0.59	4
0.05	0.32	4	0.183	0.056 ± 0.003	0.043 ± 0.002	4600
0.05	0.32	8	0.123	0.066 ± 0.005	0.053 ± 0.003	5500
0.05	0.32	32	0.074	0.0186 ± 0.0007	0.0180 ± 0.0007	14 000
0.05	0.10	16	0.094	0.0060 ± 0.0003	0.0058 ± 0.0003	43 000
0.05	0.20	16	0.094	0.0156 ± 0.0012	0.0147 ± 0.0010	17 000
0.05	0.25	16	0.094	0.0216 ± 0.0017	0.0202 ± 0.0013	12 000
0.05	0.50	16	0.094	0.1541 ± 0.0190	0.0979 ± 0.0042	1700
0.05	0.60	16	0.094	0.2537 ± 0.0317	0.1362 ± 0.0057	1000
0.05	0.70	16	0.094	0.394 ± 0.033	0.172 ± 0.006	660
0.05	1.00	16	0.094	0.476 ± 0.027	0.282 ± 0.012	550
0.10	0.10	16	0.149	0.027 ± 0.003	0.025 ± 0.003	3400
0.10	0.20	16	0.149	0.039 ± 0.001	0.029 ± 0.001	2400
0.10	0.25	16	0.149	0.042 ± 0.008	0.039 ± 0.006	2200
0.10	0.50	16	0.149	0.218 ± 0.012	0.118 ± 0.002	430
0.10	0.70	16	0.149	0.255 ± 0.021	0.123 ± 0.002	360
0.10	1.00	16	0.149	0.192 ± 0.019	0.106 ± 0.011	480

Note. The simulations are ordered in the same fashion as in Table 1. The first three columns show the parameters of the simulations, the fourth column the predicted values for $\delta(\alpha)N_0$ and the fifth and sixth columns show the values derived if we fit the theoretical formulae directly to the data of our simulations. The errors stated in those columns are the standard deviation of the fitting values and do not represent the much larger errors due to the low number statistics of the simulations. The final column gives the time needed to merge half of the subclumps $t_{1/2}$, calculated using the fitted value from the slow regime. The time is given in real time, i.e. kyr.

where, r_{merger} denotes the merger radius, i.e. the maximum distance two clumps could have to merge after the interaction, which (measured in units of the Plummer radius of the star-forming region) is a function of α . If we follow the same arguments as Fellhauer et al. (2002), i.e. we start out from the energy criterion in the impulsive approximation developed by Spitzer (1958):

$$\Delta E = \frac{1}{2} M_{\text{cl}} \left(\frac{2GM_{\text{cl}}}{r_{\text{merger}}^2 v_{\text{typ}}^2} \right)^2 \frac{3}{2} r_c^2 \quad (7)$$

and insert again $v_{\text{typ}} \approx \sqrt{2}\sigma_{\text{pl}}$, $r_c = 3/2R_{\text{pl}}$ and take into account that the two clusters will get gravitationally focused (Binney & Tremaine 1987), we arrive at the following expression:

$$\begin{aligned} \delta(\alpha)N_0 &= \left(\frac{2048}{3\pi^2} \right)^{1/2} \frac{\alpha}{\gamma^2} \left[1 + \left(\frac{8192}{27\pi^2} \right)^{1/4} \frac{1}{\sqrt{N_0\alpha}} \right], \\ &= 8.317 \frac{\alpha}{\gamma^2} \left(1 + \frac{2.355}{\sqrt{N_0\alpha}} \right), \end{aligned} \quad (8)$$

which gives with $\gamma = 4.0 \pm 0.5$ the values for $\delta(\alpha)N_0$ shown in Table 2. γ is the mean of the projected radii of the outermost subclump in the realizations of the initial conditions, in units of $R_{\text{pl}}^{\text{sc}}$.

The change between the very fast and not so fast regime takes place at a low α -value of <0.02 .

Our merger criterion (i.e. when do we regard two subclumps as merged or a subclump with the merger object) is set up in the following way: if two clumps collide with each other and their centres of density do not separate more than a certain radius r_{max} for the rest of the simulation then we regard the two clusters as merged. We favour a distance criterion to an energy criterion because all clusters are bound to each other to begin with and in later stages

we already have a merger object in the centre, which complicates the process. This merger object, which is somewhat larger than the initial clusters, is also the reason to choose a rather large r_{max} . From hundreds of simulations, we deduce that $r_{\text{max}} = R_{\text{cut}}$, where R_{cut} is the cut-off radius of our single clumps, is a good choice for identifying two clumps as merged. It is small enough that the two single clumps do not separate from each other anymore and large enough to account for merger events with the central merger object as well.

4 RESULTS

4.1 Standard model

We begin by discussion the results for our standard model. In Fig. 1, we show how the number of star clusters decreases with time. According to the prediction of Fellhauer et al. (2002), the number should decrease exponentially with time ($\alpha > 0.02$). The data points can be nicely fit with an exponential decrease with $\eta_{\text{fit}} = 0.076 \pm 0.003$ with a reduced χ^2 of 1.00 [dot-dashed (blue) line in Fig. 1]. This value is lower than the prediction of $\eta_{\text{predict}} = 0.2$, i.e. the merging happens more slowly than predicted. If we use instead the prediction of the ‘slow’ regime, we obtain the solid (green) line in Fig. 1. This line seems to fit the data also. If we determine the fitted value of δN_0 for our data, we get $(\delta N_0)_{\text{fit}} = 0.10 \pm 0.01$ with a χ^2 of 2.78. This value is in very good agreement with the prediction of the α -dependent theory of $(\delta N_0)_{\text{predict}} = 0.094$. It seems that the prediction of the old theory works well, if we shift the transition value of α from the ‘slow’ to the ‘fast’ regime to a higher value. If we check the velocity criterion formula (equation 4), we see (with

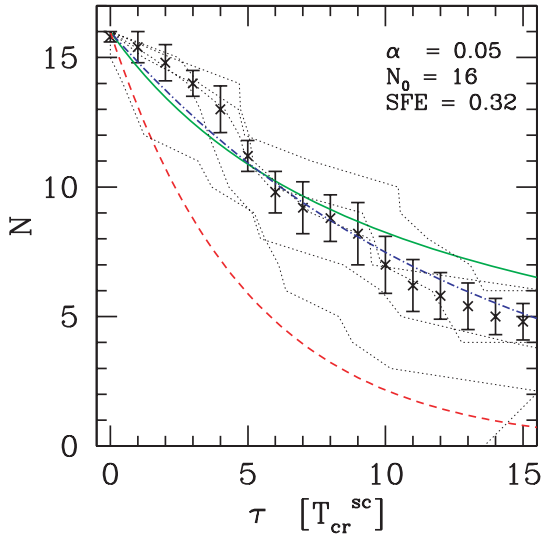


Figure 1. Our standard model. Data points with error bars show the mean values derived out of five simulations with different random seeds. The results of each of the simulations are shown as dotted lines. Dashed line (red) shows the analytical curve according to a ‘fast’ exponential decrease, solid (green) line shows the analytical curve according to the α -dependent ‘slow’ theory and dot-dashed (blue) line shows the fitted line according to an exponential decrease.

our choice of N_0 and ϵ) that $\alpha \leq 0.07$ ensures that the subclumps merge.

Going back from our dimensionless time τ ($T_{\text{cr}}^{\text{sc}} = 260$ kyr) to the real time t , we see that the majority of subclumps merge within 2–3 Myr, i.e. faster than any supernova explosion will occur and

blow out the remaining gas from the star-forming region. The model shows that by that time one already has a bound, nearly spherical merger object in the centre of the star-forming region.

We now have to find out why, and where, we have to switch from the very fast α -independent regime to the slower (but still fast) α -dependent theory. This is also interesting in the light of low-mass star clusters with 10^3 – 10^4 stars, in which the gas removal happens even faster through stellar feedback of O stars. An example of such an object would be the Orion Nebula cluster which has an age of 0.5–1.5 Myr and has already blown out most of its natal material (Kroupa et al. 2001). We therefore perform a suite of simulations with varying α , N_0 and ϵ .

4.2 Parameter Study

In Figs 2 and 3, we show the results for the parameter survey. In the left-hand panels of Fig. 2, we varied the value of α . It shows that as long as $\alpha \leq 0.2$ the slow regime fits the data points well. Only if α becomes very large (≈ 0.2) does the faster exponential decrease seem to take over. Finally, if the filling factor is as large as $\alpha = 0.5$, most of the clumps overlap at the start of the simulation and the clumps do not separate but stick together and form a cluster from the start [small (blue) crosses in the top-left panel]. This general behaviour can be understood in terms of our velocity criterion, which tells us that as long as the filling factor is smaller than $\alpha \approx 0.07$ merging between the clumps is possible. But, by the time this threshold is reached, the filling factor is high enough for the clumps to form a central merger object from the start and the ‘fast’ regime takes over.

If we keep α and ϵ constant and only vary N_0 , the merging should happen according to the ‘slow’ regime with only a slight dependency on N_0 . The right-hand panels of Fig. 2 show this behaviour nicely,

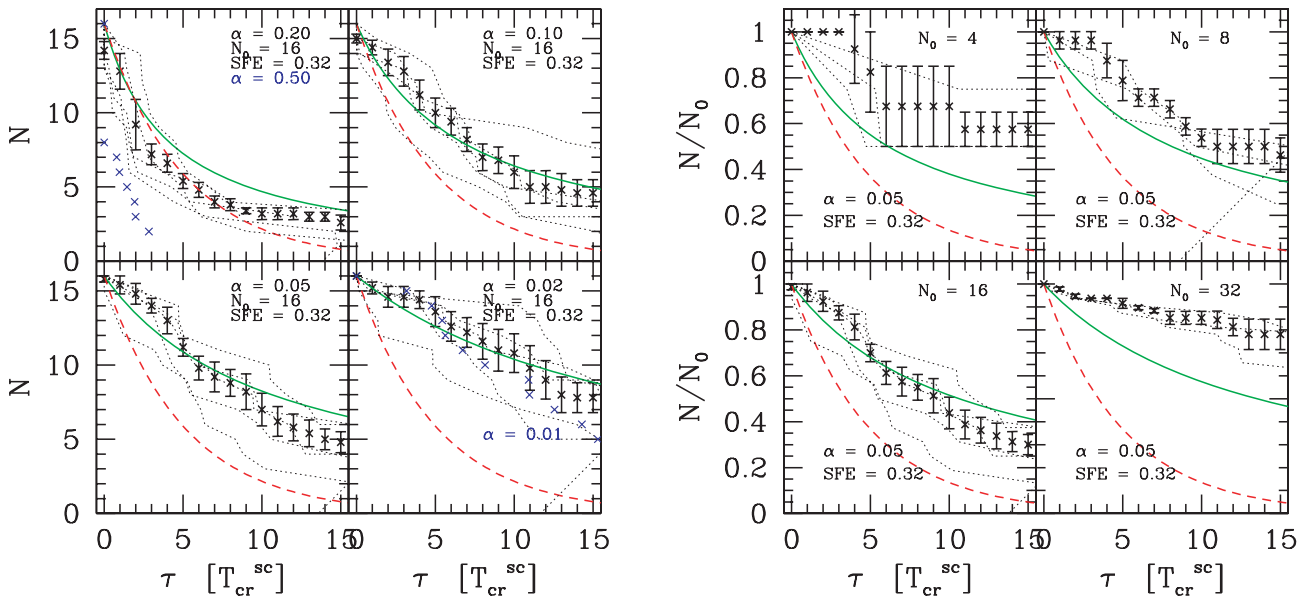


Figure 2. Left-hand panel: results of our simulations with varying values of α . Solid (green) line shows the predicted decrease according to the ‘slow’ regime, while the dashed (red) curve gives the prediction of the ‘fast’ regime. The simulations follow the ‘slow’ regime except for very high values of $\alpha \geq 0.2$. In the case of $\alpha = 0.5$ [small (blue) crosses] in the top-left panel, all clumps overlap from the beginning and merge immediately (single simulation). The light (blue) crosses in lower-right panel show a single simulation with $\alpha = 0.01$, which also follow the slow regime. Right-hand panel: results of our simulations with varying N_0 . The results show that the decrease in numbers is fairly independent of N_0 and that the ‘slow’ regime [solid (green) lines; dashed (red) lines show the ‘fast’ regime] fits the data reasonably well (simulations with only four clumps suffer from ‘very low number statistics’) as long as the number of clumps are below a certain threshold which is reached at $N_0 = 32$ (see the main text for explanation). In both sets of panels, dotted lines are the results of the individual simulations.

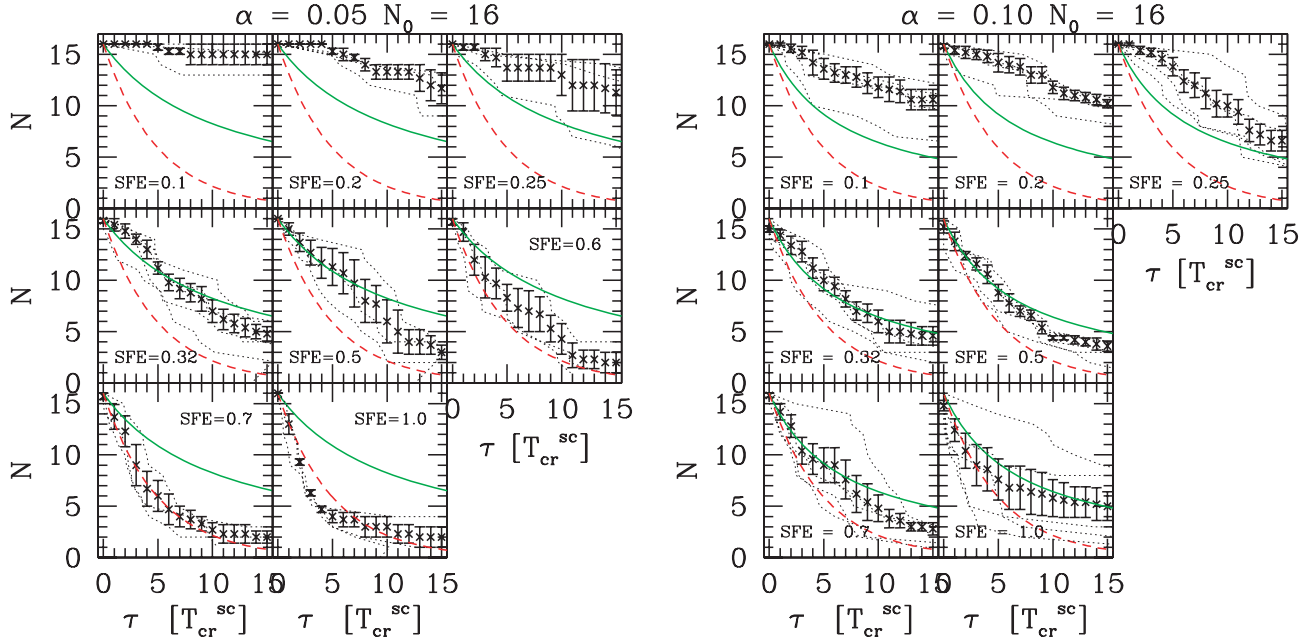


Figure 3. Results of our simulations with different SFEs. Left-hand panel: simulations with $\alpha = 0.05$. Right-hand panel: simulations with $\alpha = 0.1$. The data points are the mean number of clusters after τ crossing times out of all simulations with the same parameters. Solid (green) line is the analytical curve of the ‘slow’ regime, dashed (red) line is the analytical curve for the fast regime. Dotted lines represent each of the single simulations. One clearly sees that by varying ϵ the results show three different regimes of the merging behaviour (see the main text for explanation).

except for the bottom-right panel, when $N_0 = 32$. Here, it seems that the clumps do not merge at all. Again, this becomes clear with a look at equation (4). Inserting the constant values of ϵ and α , it results that $N_0 \leq 22$ to allow the clumps to merge. This means that by keeping all other parameters constant and just dividing the (constant) total mass in stars into more and more sub-clumps, we enter the regime where the low-mass clumps cannot absorb enough orbital energy during an encounter to merge. Merging in this regime is well suppressed and processes like destruction of the clumps due to the interactions take over.

Finally, we keep α and N_0 constant and vary the SFE ϵ . The results are shown in Fig. 3 for two values of α . Using the fitted values for δN_0 from Table 2, the data suggest a strong dependency of δN_0 on ϵ : $\delta N_0 \propto \epsilon^2$. But a closer look reveals that we rather have to deal with three different regimes. The first regime is governed by a strong background potential and almost no clumps merging. Again the mass of a single clump is too low for the clump to absorb enough energy from the orbital motion into internal energy for merging to happen, i.e. the velocity criterion fails. If, in the $\alpha = 0.05$ case (left-hand panels), the SFE is higher than $\epsilon > 0.25$, the ‘slow’ α -dependent theory takes over and fits the data nicely. This again supports our velocity criterion which tells us that $\epsilon \geq 0.24$ is required for the clumps to be massive enough to allow merging. If the SFE is higher than approximately $\epsilon = 0.5$ then the ‘fast’ regime takes over, i.e. the central clumps are able to form a merger object immediately and clumps merge with the central object.

In the right-hand panels of Fig. 3, we see the same experiments for a higher value of $\alpha = 0.1$. On a first glance, one should expect that in this case the merging should happen faster, but the velocity criterion tells a different story. If we increase the filling factor by reducing the size of the star-forming region (by keeping all other quantities constant), we raise the velocity dispersion of the clumps in the region and therefore make it more difficult for them to merge. Our simple velocity criterion (equation 4) gives us a transition value

of $\epsilon \geq 0.47$ while in our simulations we see that this transition has to be in the region of $\epsilon \approx 0.3$. Also the ‘fast’ regime is reached only at a higher SFE value of $\epsilon \geq 0.7$.

As a result of our parameter study, we deduce that even though the simple geometrical theory of Fellhauer et al. (2002) does not account for any background potential it is still applicable, with some limitations. The velocity criterion of equation (3) used in Fellhauer et al. (2002) gives (translated into the values important in this study – equation 4) a good hint for which part of the parameter space the theory, especially the ‘slow’ regime, is valid. It still needs to be established when the transition between the ‘slow’ and the ‘fast’ regime sets in. From our parameter study, we can conclude that α and ϵ are antiproportional to each other. However, the derivation of a general theory to explain the precise locations of the transition values of the parameters is postponed to a much wider study of the parameter space.

To connect our theoretical study with actual observations, we included in the last column of Table 2 the real time taken for half of the subclumps to merge, which results already in a prominent merger object, taking the values of Table 1. This shows that for our set of parameters for the star-forming cloud one can indeed find configurations that form a merger object even before the stars manage to expel the gas via stellar winds and very long before the first supernova is expected. More generally, the way to deduce this merging time for any given initial conditions is first to calculate δN_0 : the ‘half-merger time’ in crossing times of the star-forming region is just the inverse of this number. Multiplying this number with the crossing time in years gives then the final answer.

As a final remark, one should keep the statistical nature of our results in mind. We use only 16 clumps to represent the distribution of clumps in the star-forming region. In such random realizations, it is very likely that even though we use a large filling factor, i.e. a high central concentration of clumps, the random numbers give us a realization where most of the clumps are outside the central

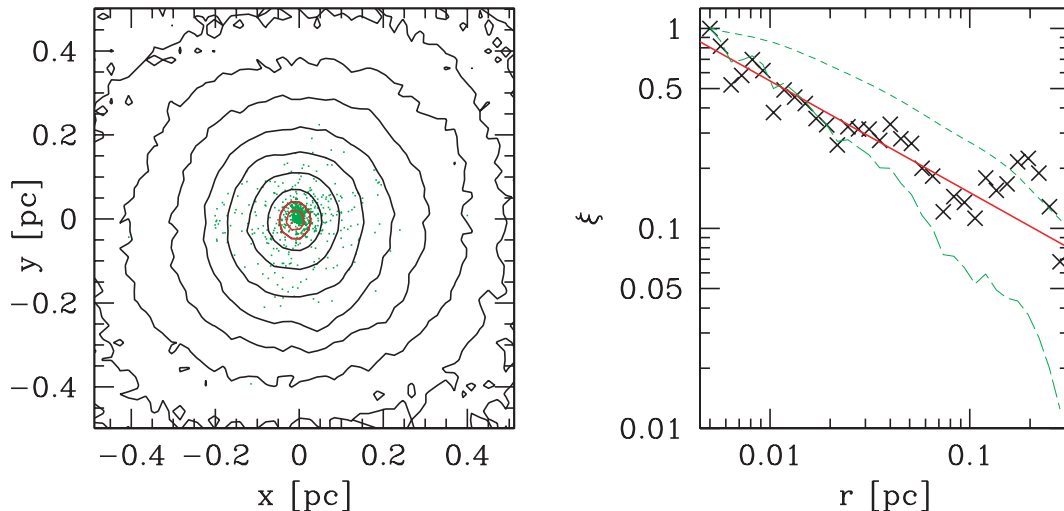


Figure 4. Left-hand panel: contour plot of the final merged cluster of one of our simulations. Overplotted as (green) dots are the positions of the 50 initially lowest energy ‘marked’ stars of each clump. Right-hand panel: the ratio ξ (crosses) between the surface-density profile of the marked stars and all stars of the merger object (normalized to 1) with the solid (red) line showing the power-law fit. The dashed (green) lines show the two profiles (also normalized to 1 in the centre) with the short dashed line showing all particles and the long dashed line the lowest (initially) energy particles only.

area and therefore act like a distribution with a much lower value of the filling factor. Also, the opposite can be true. Furthermore, by repeating the experiment with the same set of parameters only three to five times we get closer to a mean representation of our input parameters, but we also introduce extra noise to our study. In the figure panels of this manuscript, we show the behaviour of the single simulations as thin dotted lines to illustrate how differently random realizations of the same parameters can behave.

4.3 Mass Segregation

We mark the 50 innermost particles ($< 1 R_{pl}$) with the lowest energy in each subclump and locate them in the final merger object. As expected, they appear to end up in the centre of the merger object (see Fig. 4, top panel). To check if this is not merely a visual appearance due to the steep profile of the merger object, we derived the ratio of the surface density of the central particles to the surface density of all particles. As shown in the middle panel of Fig. 4, this ratio (ξ ; here normalized to unity in the centre) declines as a shallow power law with index $n = -0.56 \pm 0.04$. This shows that indeed mass-segregated stars in the centre of the subclumps end up again in the centre of the merger object.

This process is a collective effect based on phase-space arguments only and is not due to two-body relaxation effects. Using a particle-mesh code for our simulations means that the effects of two-body relaxation are almost completely switched off. The signal is smeared out, due to the fact that we only choose particles according to their position and not simultaneously if they have a velocity which keeps them in the centre, which is the case with massive, segregated stars and disruptive effects of close encounters of unmerged subclumps with the merger object. This means that the effect that central particles of subclumps end up in the centre of the merger object is not a process which requires two-body relaxation but rather a phase-space argument. Still the results would be more pronounced if we would have used a direct N -body code, allowing for two-body relaxation. This result nicely confirms and even strengthens the results of McMillan et al. (2007), who found that mass-segregated clumps form a mass-segregated star cluster.

4.4 Infant mortality

Infant mortality is one of the major problems in forming star clusters: How can star clusters survive their gas-expulsion phase without getting completely destroyed? Theoretical work predicts that the SFE has to be $\epsilon > 0.33$ if the gas is lost instantaneously to retain a small bound core of a surviving cluster. There are several effects which can help to reduce this transition value and therefore help star clusters to survive their formation process.

First, if one takes into account internal evolution by simulating the cluster with an actual initial mass function with heavy stars sinking very fast to the centre, leading to a compact core, this value can be reduced slightly (see experiments in Boily & Kroupa 2003a,b). Furthermore, it takes some time until the gas is removed from the cluster and the stars adapt to the change in potential. This helps especially very small star clusters (without massive stars) and very massive clusters (long gas-expulsion time). If star clusters do not form in isolation but in a star cluster complex, the merging of the star clusters also helps to retain a massive star cluster in the form of the merger object.

Here, we add another mechanism which helps to overcome infant mortality. The time-scale of the merging in our standard model is very fast (even though it is the ‘slow’ regime). Within 2–3 Myr, we see a merger object (star cluster) in the centre. Because the clumps have formed all over the star-forming region and are now together in the centre, while the gas is decoupled from this merging process, the ‘effective’ SFE of the merged star cluster, i.e. the ratio between stars and total mass inside the merger object (not to be confused with the effective SFE as usually found in the literature Goodwin 2008), is higher than the overall efficiency of the parent cloud. The star cluster should therefore survive instantaneous gas expulsion better.

To show this, we took the end-point of one of our merger simulations and removed the background potential instantaneously. The overall SFE of 0.32 should not allow the star cluster to survive, especially if modelled with a code which neglects internal evolution. But, Fig. 5 shows that on the contrary we remain with a bound star cluster containing about 40–50 per cent of its initial mass. This can

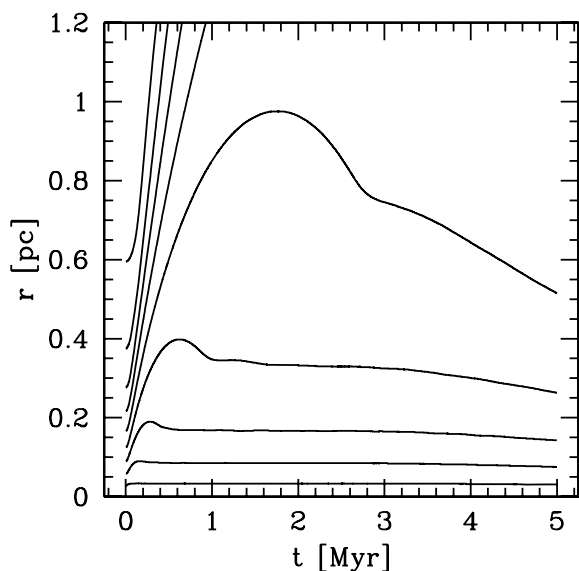


Figure 5. Lagrangian radii of one of our standard simulations after removing the background potential (gas) instantaneously at the start of the simulation. One clearly sees that about 40–50 per cent of the cluster remains bound.

be explained by looking at the stars-to-gas ratio within the half-mass radius of our merger object. Here, we see that by keeping the background (gas) potential constant the ‘effective’ SFE would have been of the order of 44 per cent (compare with Adams 2000).

One can now argue that the gravitational pull of the newly formed star cluster would also collect some of the remaining gas. But, we already start with a very simplistic realization of the background potential which is a strongly centrally concentrated Plummer model, allowing us to access all quantities analytically, being much more concentrated than a star-forming region would be. So, we indeed fulfill this criterion from the start.

5 CONCLUSIONS

In this study, we tried to find out on which time-scales stars forming in clumps inside a star-forming region merge and form an embedded star cluster. We have shown that the analytical description developed by Fellhauer et al. (2002) for the larger scale of merging star clusters inside a cluster complex can be adopted for this problem also.

By introducing a background potential, mimicking the remaining gas, the basic theory need not be changed at all, although a shift of the critical values of the parameters which separate particular merging behaviours is required. In the old study, already a low filling factor of $\alpha \geq 0.02$ allowed the star clusters to merge very fast, decreasing their number exponentially. The presence of a background potential shifts this limit to rather high α values of about 0.2 due to the larger cluster–cluster velocities. This can be understood in the sense that the theory itself is geometrical and velocity independent, because all velocities were within a certain range which allows for this fast merging. So, at each crossing time the same fraction of remaining clusters/clumps is able to merge with the central object. In the presence of a background potential, the relative velocities of the clusters/clumps are higher, although the clusters have the same ability to absorb energy from the flybys. At any given time, this therefore reduces the number of clusters with velocities suitable for merging.

Nevertheless, the old theory for the very low α regime (i.e. when the filling factor is so low that merging preferentially happens between two clusters/clumps at a time) provides a very good fit to the data. In this regime, the number of clusters decreases according to $1/1 + \tau$. For our standard model, this translates into a merging time for almost all of the subclumps which is much shorter than the time-scale until the first supernova explodes. Under these conditions, a virialized star cluster forms well before gas expulsion, driven by supernovae, occurs. For intermediate-mass clusters containing between about 10^3 and 10^4 stars, gas expulsion occurs earlier and the requirement that subclustering disappears by the time the gas is expelled implies stringent constraints on the configuration of the subclusters. Nevertheless, such configurations are found in our parameter study. The new, hierarchically formed, embedded star cluster is then able to survive the gas expulsion much more easily than a monolithically formed cluster would have done, because the ‘effective’ SFE at its location is much higher than the overall SFE of the region in which it formed.

Finally, this study has confirmed and strengthened the findings of McMillan et al. (2007) that mass-segregated clumps form mass-segregated clusters. Even though our method does not allow for mass-segregation at all, we are able to flag the lowest energy (i.e. the most bound) particles in the centre of each clump and locate them in the final merger object. We show that these particles are more centrally concentrated than the other particles. This shows that this process is governed by simple phase-space arguments and is not solely due to two-body relaxation. As we have shown, it is not an effect of mass segregation that massive, already mass-segregated (within their native clump) stars end up in the central region of the newly formed cluster.

ACKNOWLEDGMENTS

MF would like to acknowledge financial support from STFC in the UK at the beginning of the project and now through FONDECYT, Chile. The authors also would like to thank C. Clarke for useful comments. MIW acknowledges the Royal Society for support.

REFERENCES

- Adams F. C., 2000, *ApJ*, 542, 964
- Baumgardt H., Kroupa P., Parmentier G., 2008, *MNRAS*, 384, 1231
- Binney J., Tremaine S., 1987, *Galactic Dynamics*. Princeton Univ. Press, Princeton, NJ
- Boily C. M., Kroupa P., 2003a, *MNRAS*, 338, 665
- Boily C. M., Kroupa P., 2003b, *MNRAS*, 338, 673
- Bonnell I. A., Bate M. R., Vine S. G., 2003, *MNRAS*, 343, 413
- Burkert A., Bodenheimer P., 2000, *ApJ*, 543, 822
- Clark P. C., Bonnell I. A., 2004, *MNRAS*, 347, L36
- de Grijs R., Goodwin S. P., 2008, *MNRAS*, 383, 1000
- Fellhauer M., Kroupa P., Baumgardt H., Bien R., Boily C. M., Spurzem R., Wassmer N., 2000, *New Astron.*, 5, 305
- Fellhauer M., Baumgardt H., Kroupa P., Spurzem R., 2002, *Celest. Mech. Dyn. Astron.*, 82, 113
- Gerhard O. E., Fall S. M., 1983, *MNRAS*, 203, 1253
- Geyer M. P., Burkert A., 2001, *MNRAS*, 323, 988
- Gieles M., Bastian N., 2008, *A&A*, 482, 165
- Goodwin S. P., 1997, *MNRAS*, 284, 785
- Goodwin S. P., 1998, *MNRAS*, 294, 47
- Goodwin S. P., 2008, preprint (arXiv:0802.2207)
- Goodwin S. P., Whitworth A. P., 2004, *A&A*, 413, 929
- Goodwin S. P., Nutter D., Kroupa P., Ward-Thompson D., Whitworth A. P., 2008, *A&A*, 477, 823

- Johnstone D., Wilson C. D., Moriaty-Schieven G., Joncas G., Smith G., Gregersen E., Fich M., 2000, *ApJ*, 545, 327
- Klessen R., Burkert A., 2001, *ApJ*, 549, 386
- Kroupa P., 2005, in Turon C., O’Flaherty K. S., Perryman M. A. C., eds, *The Three-Dimensional Universe with Gaia*, ESA-SP 576. ESA Publications, Noordwijk, p. 629
- Kroupa P., Aarseth S., Hurley J., 2001, *ApJ*, 549, 386
- Lada C. J., Lada E. A., 2003, *ARA&A*, 41, 57
- MacLow M., Klessen R., 2004, *Rev. Mod. Phys.*, 76, 125
- McMillan S. L., Vesperini E., Portegies Zwart S. F., 2007, *ApJ*, 655, L45
- Parmentier G., Goodwin S. P., Kroupa P., Baumgardt H., 2008, *ApJ*, 678, 347
- Scally A., Clarke C., 2002, *MNRAS*, 334, 156
- Sensui T., Funato Y., Makino J., 2000, *PASJ*, 51, 1
- Spitzer Jr. L., 1958, *ApJ*, 127, 17
- Tilley D. A., Pudritz R. E., 2004, *MNRAS*, 353, 769
- Whitmore B. C., Zhang Q., Leitherer C., Fall S. M., 1999, *AJ*, 118, 1551

This paper has been typeset from a $\text{\TeX}/\text{\LaTeX}$ file prepared by the author.